



MID-AMERICA TRANSPORTATION CENTER

Report # MATC-MS&T: 194

Final Report
WBS:25-1121-0003-194

UNIVERSITY OF
Nebraska
Lincoln

K-STATE
Kansas State University

KU
THE UNIVERSITY OF
KANSAS

MISSOURI
S&T
University of
Science & Technology

U LINCOLN
University

 University of Missouri

IOWA STATE
UNIVERSITY


THE UNIVERSITY OF IOWA

Splice Performance Evaluation of Enamel-Coated Rebar for Structural Safety

G.D. Chen, Ph.D., P.E., F .ASCE, F .Sei

Professor and Robert W. Abnett Distinguished Chair in Engineering
Department of Civil, Architectural, and Environmental Engineering
Missouri University of Science and Technology

C.L. Wu, Ph.D. candidate

Graduate Research Assisstant
Department of Civil, Architectural, and Environmental Engineering
Missouri University of Science and Technology

MISSOURI
S&T
University of
Science & Technology

2014

A Coopertative Research Project sponsored by
U.S. Department of Tranportation-Research, Innovation and
Technology Innovation Administration

MATC

The contents of this report reflect the views of the authors, who are responsible for the facts and the accuracy of the information presented herein. This document is disseminated under the sponsorship of the Department of Transportation University Transportation Centers Program, in the interest of information exchange.
The U.S. Government assumes no liability for the contents or use thereof.

Splice Performance Evaluation of Enamel-Coated Rebar for Structural Safety

G.D. Chen, Ph.D., P.E., F.ASCE, F.SEI

Professor and Robert W. Abbett Distinguished Chair in Civil Engineering
Department of Civil, Architectural, and Environmental Engineering
Missouri University of Science and Technology

C.L. Wu, Ph.D. Candidate

Graduate Research Assistant

Department of Civil, Architectural, and Environmental Engineering
Missouri University of Science and Technology

A Report on Research Sponsored By

Mid-America Transportation Center

University of Nebraska–Lincoln

US DOT Research and Innovative Technology Administration

Center for Infrastructure Engineering Studies

Missouri University of Science and Technology

July 2014

Technical Report Documentation Page

1. Report No. 25-1121-0003-194	2. Government Accession No.	3. Recipient's Catalog No.	
4. Title and Subtitle Splice Performance Evaluation of Enamel-coated Rebar for Structural Safety		5. Report Date July 2014	
		6. Performing Organization Code	
7. Author(s) G.D. Chen and C.L. Wu		8. Performing Organization Report No. 25-1121-0003-194	
9. Performing Organization Name and Address Mid-America Transportation Center 2200 Vine St. PO Box 830851 Lincoln, NE 68583-0851		10. Work Unit No. (TRAIS)	
		11. Contract or Grant No.	
12. Sponsoring Agency Name and Address Research and Innovative Technology Administration 1200 New Jersey Ave., SE Washington, D.C. 20590		13. Type of Report and Period Covered Final Report, July 2012 - June 2014	
		14. Sponsoring Agency Code MATC TRB RiP No. 17139 (this listing includes the scope of both MATC project numbers associated with this project)	
15. Supplementary Notes			
16. Abstract This report summarizes the findings and results from an experimental study of vitreous enamel coating effects on the bond strength between deformed rebar and normal strength concrete. A total of 24 beam splice specimens were tested under four-point loading with four parameters investigated: bar size, lap splice length, coating, and confinement conditions. As the splice length increases, the ratio of bond strength between coated rebar and black rebar first increases from 1.0 to a maximum value of 1.44, and then decreases to 1.0. The maximum bond strength ratio corresponds to the near initial yielding of coated rebar. On the average, enamel coating can increase the bond strength of steel rebar in concrete by approximately 15%. A coating factor of 0.85 is thus recommended to take into account the enamel coating effect in lap splice designs, according to ACI and AASHTO bond strength equations.			
17. Key Words Enamel coating, deformed rebar, bond strength, coating factor		18. Distribution Statement	
19. Security Classif. (of this report) Unclassified	20. Security Classif. (of this page) Unclassified	21. No. of Pages 29	22. Price

Table of Contents

Acknowledgements	vi
Disclaimer	vii
Abstract	viii
Executive Summary	ix
Chapter 1 Introduction	1
Chapter 2 Experimental Program.....	3
2.1 Materials	3
2.2 Test Specimens	7
2.3 Test Setup and Instrumentation	8
Chapter 3 Results and Discussion.....	10
3.1 Data Analysis	10
3.2 Crack Pattern and Failure Details	11
3.3 Load-Deflection and Load-Strain Curves	16
3.4 Bond Ratio	20
3.5 Coating Factor for Enamel-Coated Rebar.....	22
Chapter 4 Conclusions	25
References	27

List of Figures

Figure 2.1 (cont.) Stress-strain relationship for grade 420 no.19 and no.25 rebar: before and after heat treatment.....	4
Figure 2.2 Reinforcement details of series A-H (all units in mm).....	7
Figure 2.3 Reinforcement details of series I-L (all units in mm).....	8
Figure 3.1 Crack pattern in constant moment region of series A.	122
Figure 3.2 Crack pattern in constant moment region of series I.....	133
Figure 3.3 Crack pattern in constant moment region of series I.....	144
Figure 3.4 Crack pattern in constant moment region of series I.....	155
Figure 3.5 Load-deflection and load-strain curves for series C.....	166
Figure 3.6 Load-deflection and load-strain curves for series D.....	177
Figure 3.7 Load-deflection and load-strain curves for series E.....	177
Figure 3.8 Load-deflection and load-strain curves for series I.....	177
Figure 3.9 Load-deflection and load-strain curves for series K.....	188
Figure 3.10 Load-deflection and load-strain curves for series L.....	188
Figure 3.11 Bond ratio comparison between epoxy coated and enamel-coated rebar.....	21
Figure 3.12 Ratio of test to predicted for series associated with splitting failure.....	233

List of Tables

Table 2.1 Splice specimen properties and test results.....	5
Table 3.1 Bond stress prediction with various design equations.....	23

Acknowledgements

Financial support for this study was provided in part by Mid-America Transportation Center under Contract Agreement No. 25-1121-0003-194 and by the National Science Foundation under Award No. CMMI-0900159. The authors would like to thank Brian Swift, Gary Abbott, Jason Cox and John Bullock for their assistance with various experimental setups. Steel rebar was coated with enamels by Pro-Perma Engineered Coatings in Rolla, MO. The findings and opinions expressed in this report are those of the authors only and do not necessarily represent those of the sponsors.

Disclaimer

The contents of this report reflect the views of the authors, who are responsible for the facts and the accuracy of the information presented herein. This document is disseminated under the sponsorship of the U.S. Department of Transportation's University Transportation Centers Program, in the interest of information exchange. The U.S. Government assumes no liability for the contents or use thereof.

Abstract

This report summarizes the findings and results from an experimental study of vitreous enamel coating effects on the bond strength between deformed rebar and normal strength concrete. A total of 24 beam splice specimens were tested under four-point loading with four parameters investigated: bar size, lap splice length, coating, and confinement conditions. As the splice length increases, the ratio of bond strength between coated rebar and black rebar first increases from 1.0 to a maximum value of 1.44, and then decreases to 1.0. The maximum bond strength ratio corresponds to the near initial yielding of coated rebar. On the average, enamel coating can increase the bond strength of steel rebar in concrete by approximately 15%. A coating factor of 0.85 is thus recommended to take into account the enamel coating effect in lap splice designs, according to ACI and AASHTO bond strength equations.

Executive Summary

This report summarizes the findings and results of an MATC research project No. 25-1121-0003-194. The project was focused on understanding of the splice mechanism and capacity of enamel-coated rebar in concrete beams. Reinforced concrete structures often have congested rebar cages in joint areas. The congested areas affect the workmanship of construction workers during concrete casting so that the concrete quality is potentially compromised. They also require longer time to complete casting. Therefore, reducing the required number of rebar or required length in joint areas is quite meaningful in practice.

A total of 24 beam splice specimens were tested under four-point loading with four parameters investigated: bar size, lap splice length, coating, and confinement conditions. As the splice length increases, the ratio of bond strength between coated rebar and black rebar first increases from 1.0 to a maximum value of 1.44 and then decreases to 1.0. The maximum bond strength ratio corresponds to the near initial yielding of coated rebar. On the average, enamel coating can increase the bond strength of steel rebar in concrete by approximately 15%. A coating factor of 0.85 is thus recommended to take into account the enamel coating effect in lap splice designs according to ACI and AASHTO bond strength equations.

Chapter 1 Introduction

Coatings have become one of the most direct and effective ways to protect steel reinforcement from corrosion when reinforced concrete (RC) structures are exposed to corrosive environments. Commercially available coating systems, such as Fusion-Bonded Epoxy (FBE), have been widely applied to steel rebar. However, previous studies [1-7] showed that a significant reduction of steel-concrete bond strength is induced by the FBE coating.

Depending on the application condition, a coating factor of 1.2 or 1.5 was thus adopted for epoxy coated bars in the ACI Building Code [8] and AASHTO Bridge Specifications [9]. Although the reduction factor in design code is likely conservative [3-5], an average of 15% reduction in bond strength may not be far from reality [6]. The resulted increase in development length compared to black rebar can not only increase the cost of materials, but may also compromise the quality control in construction due to rebar congestion in areas of stress concentration.

Enamel coating has recently become a viable corrosion barrier for steel rebar [10] and can be modified with chemical additives to enhance the bond strength of steel rebar in concrete. For example, calcium silicate (CS) particles taken from the Portland cement were added to enamel frits and mixed with water; the enamel slurries were successfully fused on 6.35 mm-diameter steel pins at a high temperature [11]. The CS-modified enamel coating is chemically reactive to cement. It potentially provides a smooth transition from the concrete to steel rebar in RC structures and eliminates the traditionally weak interface formed between the cement paste and the steel, as water is often trapped around the steel surface during the hydration process [12]. Yan et al. [13] found that a mixture of 50% CS particles and 50% commercial enamel (PEMCO International) by weight, referred to as 50/50 enamel coating hereafter, gave the maximum bond

strength between steel pins and mortar. Specifically, the 50/50 coating can increase the bond strength of smooth pins in mortar by over 2 times due to increased adhesion, and by over 3 times due to surface roughness, totaling over 7 times.

However, the bond strength between deformed bars and concrete in practical applications is dominated by the steel rib bearing effect on the concrete in addition to the adhesion and friction at the steel-concrete interface. Therefore, a series of experimental studies were recently initiated at Missouri University of Science and Technology to characterize the bond strength of enamel-coated reinforcement in concrete for various applications. Specifically, a local bond study of 50/50 enamel-coated rebar embedded in concrete cylinders was recently conducted and reported [14]. Overall, the bond strength of enamel-coated rebar in concrete was approximately 15% higher than that of black rebar in concrete. Forensic studies indicated that concrete debris was observed at the rib areas of steel rebar due to the increased adhesion and friction at the steel-concrete interface.

To understand how the steel-concrete bond strength of enamel-coated steel rebar is transferred from a structural component to a structural member/system, the coated and black rebar splice strengths in concrete are investigated in RC beams under four-point loading in this study. In particular, the effects of coating, rebar size, lap splice length, transverse reinforcement, and concrete strength are evaluated, and a bond strength equation is recommended for the design of RC structures containing enamel-coated reinforcement.

This report describes the experimental program, test setup, test results and discussion. It consists of four main chapters. Chapter 1 introduces the background and importance of this research. Chapter 2 details the test setup, measurement procedure, and test methodology. Chapter 3 deals with test results and discussion. Chapter 4 summarizes all the findings and conclusions.

Chapter 2 Experimental Program

Reinforcement splice is crucial to the functionality and safety of RC structures [15, 16]. In the past 70 years, beam splices were extensively tested with short splice lengths so that the bond strength associated with concrete splitting failures is evaluated as observed in most applications [17-20]. Due to the lack of data in bond strength of vitreous enamel-coated rebar in RC members, this study includes both short and long splice lengths, and evaluates both concrete splitting and steel yielding associated bond strengths.

The experimental program in this study consisted of 24 beam splice specimens: 12 reinforced with enamel-coated rebar and 12 with black rebar for comparison. The specimens were designed and tested in a series of 12 identical pairs: coated versus black. All specimens contained Class B ACI/Class C AASHTO splices [8, 9].

2.1 Materials

Reinforcing steel - Black bars used in this research conformed to the requirement of ASTM A615 Specifications [21]. Sand-blasted black bars were dipped into 50/50 enamel slurry (glass frit, clay, electrolytes, and Portland cement), heated for 2 minutes at 150 °C to drive off moisture, heated again in a gas-fired furnace to 810 °C for 10 minutes, and finally cooled to room temperature [6,7]. This firing melted the glass frit and bound it to the steel. After firing, the average thickness of enamel coatings ranged from 100 to 200 μm.

To ensure that the heat treatment process had no influence on the mechanical properties of enamel-coated rebar, both enamel-coated and black rebar (Grade 420 No.19 and No.25) were tested in tension according to ASTM A370 Specifications [22]. The stress-strain curves of two coated and two black rebar are presented in figure 2.1. Clearly, their overall difference is insignificant and the effect of high temperature treatment on the mechanical properties of the

steel rebar is negligible. Specifically, the average yield strength of the black and coated specimens is 491 MPa for No.19 rebar and 506 MPa for No.25 rebar. Grade 280 No.10 and No.13 deformed rebar were also used as transverse reinforcement in various beam specimens. Based on tensile tests, the average yielding strength is 276 MPa for No.10 rebar and 283 MPa for No.13 rebar.

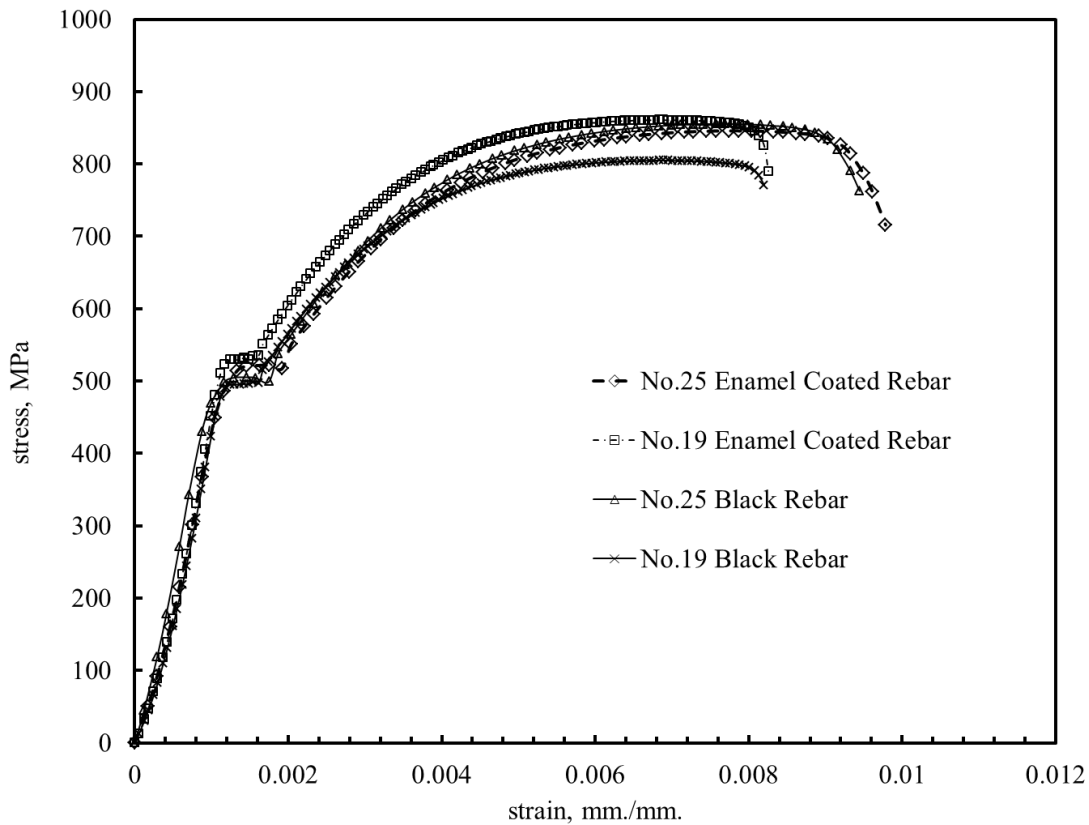


Figure 2.1 Stress-strain relationship for grade 420 no.19 and no.25 rebar: before and after treatment

Concrete - Type I Portland-cement, 19-mm coarse limestone aggregates, and natural sands were used in this study. The constituents were mixed with water at a water-cement ratio of 0.45 with no admixtures. The 28-day compressive strengths f_c' , determined by concrete cylinder tests, ranged from 27 MPa to 38 MPa as listed in table 2.1.

Table 2.1 Splice specimen properties and test results

Series	Notation	d_b (mm)	d_s (mm)	c^*/d_b	f'_c (MPa)	l_s (mm)	P_u (kN)	M_u (kN-m)	Δ_0 (mm)	f_s (MPa)	u_{test} (MPa)	$u_{test,n}$ (MPa)	Bond Ratio	Failure [†] Mode
A	6C12N	19.05	N/A	1.5	27.58	304.8	104.0	95.1	5.8	341.0	5.33	5.49	1.16	S
	6B12N	19.05	N/A	1.5	31.03	304.8	92.83	84.9	5.0	303.5	4.74	4.74		S
B	6C12T	19.05	9.525	1.5	27.58	304.8	125.1	114.4	10.9	414.4	6.47	6.67	1.14	S
	6B12T	19.05	9.525	1.5	29.65	304.8	111.9	102.3	7.6	368.6	5.76	5.83		S
C	6C16N	19.05	N/A	1.5	27.58	406.4	116.1	106.2	7.6	383.4	4.49	4.63	1.44	S
	6B16N	19.05	N/A	1.5	27.58	406.4	80.96	74.0	5.1	265.7	3.11	3.21		S
D	6C16T	19.05	9.525	1.5	31.03	406.4	135.9	124.2	14.5	444.0	5.20	5.20	1.31	S
	6B16T	19.05	9.525	1.5	31.03	406.4	102.8	94.0	7.1	337.8	3.96	3.96		S
E	6C32N	19.05	N/A	1.5	27.58	812.8	142.7	130.5	11.9	468.8	2.75	2.83	1.09	Y/S
	6B32N	19.05	N/A	1.5	37.92	812.8	141.4	129.3	12.2	464.0	2.72	2.59		Y/S
F	6C32T	19.05	9.525	1.5	27.58	812.8	148.8	136.0	15.8	487.4	2.86	2.94	1.05	Y/S
	6B32T	19.05	9.525	1.5	34.47	812.8	150.4	137.5	16.8	491.3	2.88	2.80		Y/S
G	6C36N	19.05	N/A	1.5	27.58	914.4	157.1	143.7	30.5	491.3	2.56	2.64	1.06	Y/S
	6B36N	19.05	N/A	1.5	27.58	914.4	141.9	129.7	16.0	462.0	2.41	2.48		Y/S
H	6C36T	19.05	9.525	1.5	27.58	914.4	171.0	156.3	27.7	491.3	2.56	2.64	1.00	Y/S
	6B36T	19.05	9.525	1.5	27.58	914.4	149.3	136.5	9.9	491.3	2.56	2.64		Y/S

*c = minimum concrete cover; Notation: #L##L; # = rebar size (6 and 8 for 19 mm and 25 mm in diameter); L = C for enamel-coated rebar and L = B for black rebar; ## = splice length (12, 16, 32, and 36 for 305 mm, 406 mm, 813 mm, and 914 mm in length); L = N for no transverse reinforcement and L = T for transverse reinforcement provided.

† Failure mode: S for concrete splitting; Y/S for rebar yielding prior to concrete splitting.

Table 2.1 (cont.) Splice specimen properties and test results

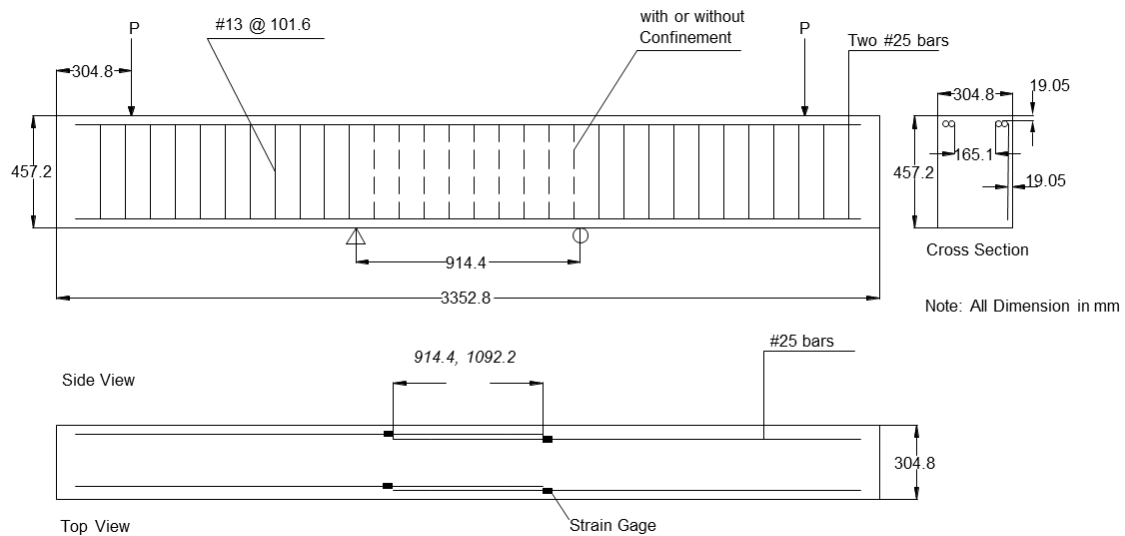
Series	Notation	d_b (mm)	d_s (mm)	c^*/d_b	f_c' (MPa)	l_s (mm)	P_u (kN)	M_u (kN-m)	Δ_0 (mm)	f_s (MPa)	u_{test} (MPa)	$u_{test,n}$ (MPa)	Bond Ratio	Failure [†] Mode
I	8C36N	25.4	N/A	1.25	27.58	914.4	247.3	226.2	20.1	480.2	3.33	3.43	1.35	S
	8B36N	25.4	N/A	1.25	31.03	914.4	186.6	170.6	7.1	365.4	2.54	2.54		S
J	8C36T	25.4	12.7	1.25	31.03	914.4	263.8	241.2	9.9	505.7	3.51	3.51	1.10	Y/S
	8B36T	25.4	12.7	1.25	37.92	914.4	250.8	229.4	11.2	482.6	3.35	3.19		S
K ⁺	8C43N	25.4	N/A	1.25	27.58	1092	238.2	196.7	9.1	475.7	2.50	2.57	1.15	S
	8B43N	25.4	N/A	1.25	27.58	1092	211.9	193.7	7.1	413.7	2.18	2.25		S
L ⁺	8C43T	25.4	12.7	1.25	27.58	1092	280.2	231.4	25.6	505.6	2.65	2.73	1.00	Y/S
	8B43T	25.4	12.7	1.25	27.58	1092	289.1	238.7	15.0	505.6	2.65	2.73		Y/S

*c = minimum concrete cover; Notation: #L##L; # = rebar size (6 and 8 for 19 mm and 25 mm in diameter); L = C for enamel-coated rebar and L = B for black rebar; ## = splice length (36 and 43 for 914 mm and 1092 mm in length); L = N for no transverse reinforcement and L = T for transverse reinforcement provided. ⁺ Bending moment was evaluated at the end of lap splices that are outside the constant moment zone.

† Failure mode: S for concrete splitting; Y/S for rebar yielding prior to concrete splitting.

2.2 Test Specimens

A total of 24 beams were prepared as shown in figures 2.2 and 2.3 with long and short splice lengths, respectively. Each beam was measured at 3353 mm long, 305 mm wide, and 457 mm deep. In the center 914 mm constant moment region of the beam, two spliced rebar were placed on the tension side under a 4-point loading system. As the first study on the use of enamel-coated rebar in a tension splice, a relatively wide range of splice lengths, from 305 mm to 1092 mm, were designed to evaluate the stress development in the coated rebar. A minimum constant moment region equal to twice the beam height was provided to ensure a negligible effect of concentrated loads on the pure flexural behavior of the beams [23].



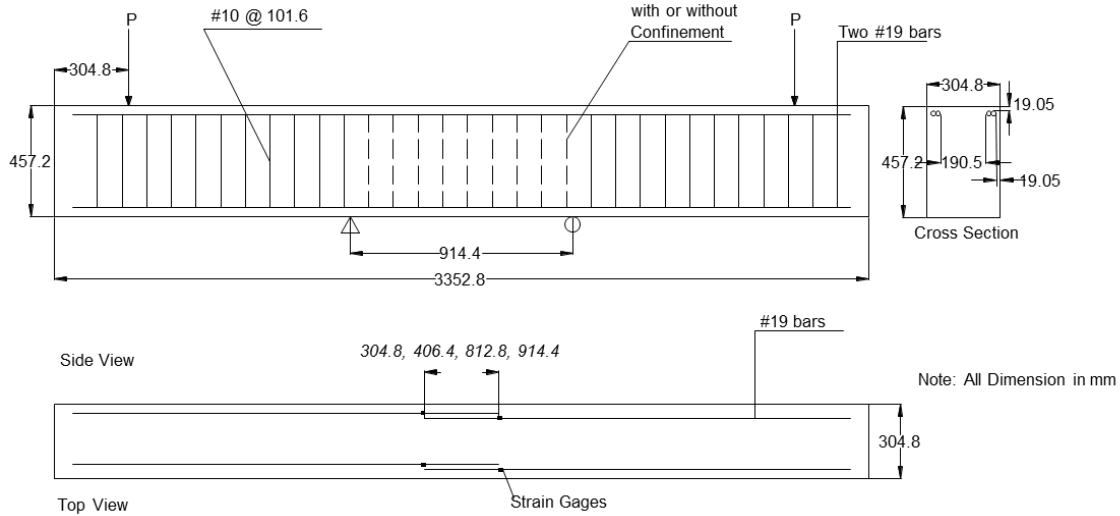


Figure 2.3 Reinforcement details of series I-L (all units in mm)

All beam specimens were cast with the splice at the bottom, but subsequently inverted for testing. As indicated in figures 2.2 and 2.3, they were reinforced with Grade 420 No.19 or No.25 rebar in the longitudinal direction, and Grade 280 No.10 or No.13 closed stirrups in the transverse direction. In the constant moment region, some specimens have no transverse reinforcement in order to study the lateral confinement effect on the splice behavior. Each beam specimen is identified with a series of numbers and letters as specified in table 2.1.

2.3 Test Setup and Instrumentation

As shown in figures 2.2 and 2.3, each specimen was tested under a four-point loading system. Two roller supports at 914 mm apart were centered about the mid-span of the beam. Two jacks at 2743 mm apart, also centered about the mid-span, were used to simultaneously load the beam with a controlled displacement rate of approximately 1.27 mm per minute until failure. In this way, the middle 914 mm of the beam was subjected to a constant moment.

Two Linear Variable Differential Transformers (LVDTs) were deployed at the two sides of each beam specimen at mid-span, and one additional LVDT was provided at each end of the

beam to monitor vertical deflections during the tests. Eight strain gages (two strain gages at one location) were also installed on the two longitudinal rebar at each end of the splice length (shown in figs. 2.2 and 2.3) to monitor the change of stress in the steel reinforcement during the tests. The average readings of strain gages at two pairs of spliced rebar were used as strain response.

Chapter 3 Results and Discussion

Among the 24 beams tested, 16 specimens failed in splitting of the concrete cover prior to the yielding of steel reinforcement, and 8 specimens experienced steel yielding prior to splitting of the concrete cover. Following is a presentation of a detailed analysis of the test data.

3.1 Data Analysis

Beams with Concrete Splitting Failure - The average bond strength was calculated using equation 1 from the calculated stress in the deformed rebar at failure. The reinforcement stress was determined from the measured strain using the stress-strain relationship of the rebar.

$$u_{avg} = \frac{A_s f_s}{\pi d_b l_d} = \frac{f_s d_b}{4l_d} \quad (1)$$

where u_{avg} is the average bond stress along the splice length, f_s is the stress in single rebar, l_d is the splice length, A_s is the cross sectional area of rebar, and d_b is the diameter of rebar.

For a direct comparison among test specimens of various concrete strengths, the average bond strength of each test was normalized to a 28-day concrete compressive strength of 31 MPa. The normalized average bond strength $u_{avg,n}$ is equal to u_{avg} multiplied by $(31/f'_c)^{1/4}$ in which f'_c represents the actual compressive strength of the concrete in MPa, and a nominal concrete strength of 31 MPa is used in this normalization (note that the use of 1/4 power in $f'_c^{1/4}$ was based on Darwin et al.[24]).

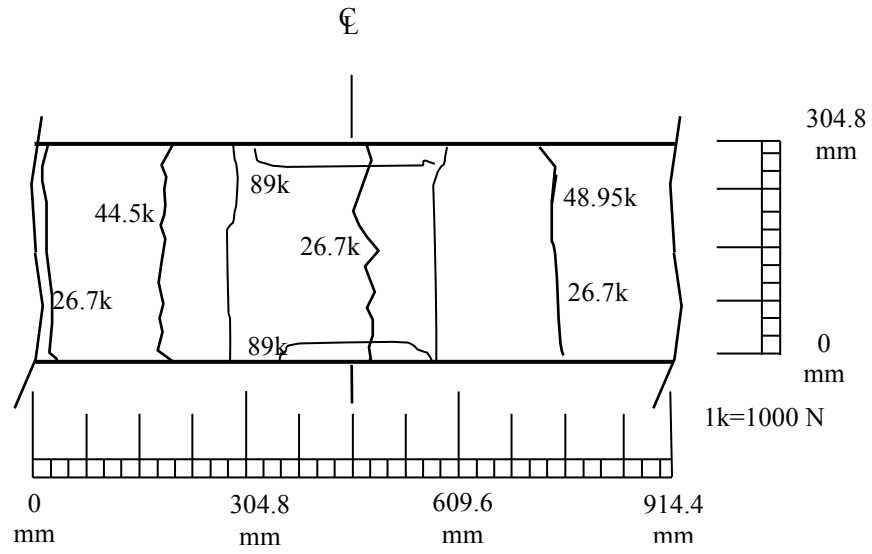
Both the original and normalized average bond strengths are listed in table 2.1. For each series of two beams, a bond ratio was then defined as the ratio of the normalized average bond strength of the coated reinforcement to the normalized average bond strength of the black rebar.

The ultimate load (P_u) and its corresponding deflection (Δ_0) for each beam are also included in table 2.1.

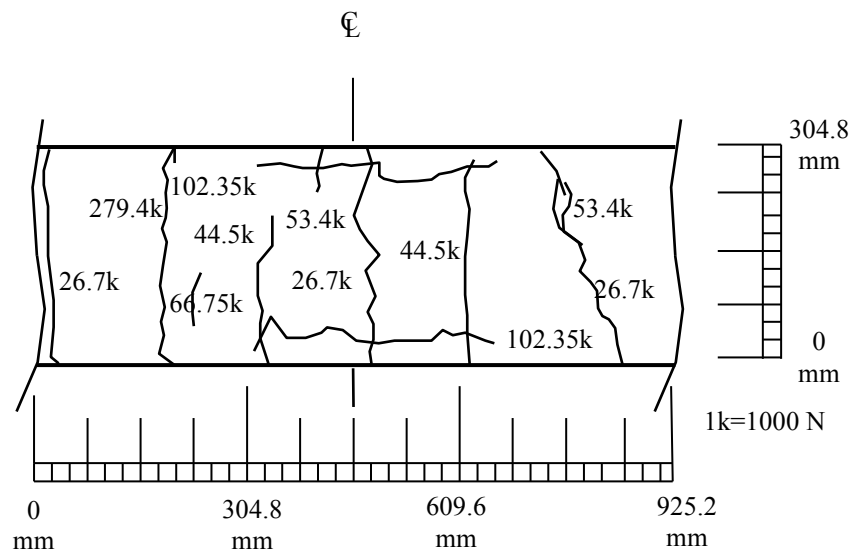
Beam with Steel Yielding Prior to Concrete Splitting - For series F, G, and L, steel yielding occurred prior to the splitting of the concrete cover in the splice region. The average bond strength was also calculated with equation 1.

3.2 Crack Pattern and Failure Details

Beams with Concrete Splitting Failure - Series A-E with No.19 reinforcement and series I-K with No.25 reinforcement all failed in concrete splitting prior to yielding of the steel reinforcement. The failure mode included concrete splitting both on the top and side covers of the beam in the splice region. Flexural cracks were initiated at various locations along the tension side and within the constant moment region of the beams. Figures 3.1 and 3.2 show two typical crack patterns on the top/tension face of the concrete cover in the splice region of the tested beams with coated and black rebar when lateral confinement was not provided in the splice region. The number given along each crack represents the load at which the crack was extended. It can be seen from figures 3.1 and 3.2 that the specimens with enamel-coated reinforcement appeared to have more transverse flexural cracks developed in the splice region, but clearly delayed the formation of longitudinal splitting cracks. The beams suddenly failed immediately after the longitudinal splitting cracks appeared on the top/tension face.

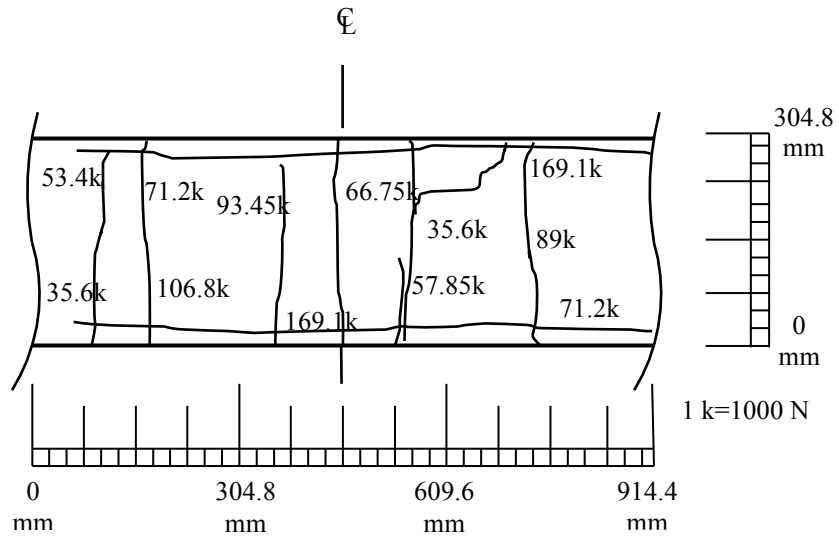


(a) 6B12N

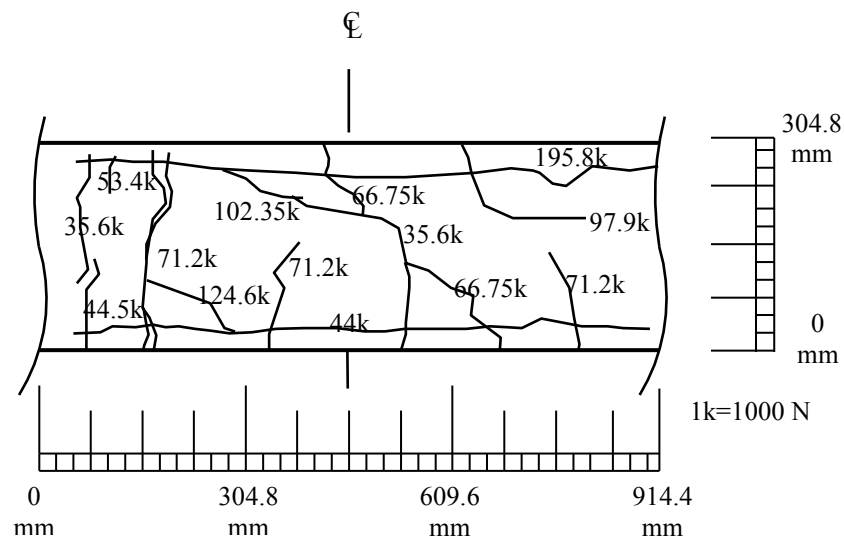


(b) 6C12N

Figure 3.1 Crack pattern in constant moment region of series A



(a) 8B36N



(b) 8C36N

Figure 3.2 Crack pattern in constant moment region of series I

As the displacement increased, the concrete splitting cracks in the splice region were significantly widened, and the concrete cover detached and could be easily removed without disturbing the surface condition of the rebar. For beams with enamel-coated reinforcement as, illustrated in figure 3.3, significant concrete residuals remained on the coating surface over the splice length, indicating a significant chemical adhesion between the coating and concrete.

Concrete crushing was also evident in the vicinity of rebar ribs, which indicated that the specimen failed in Mode 2 splitting [25]. On the contrary, for beams with black reinforcement (fig. 3.4), concrete residuals were present only at the rib-front areas due to steel bearing on the concrete.



Figure 3.3 Crack pattern in constant moment region of series I

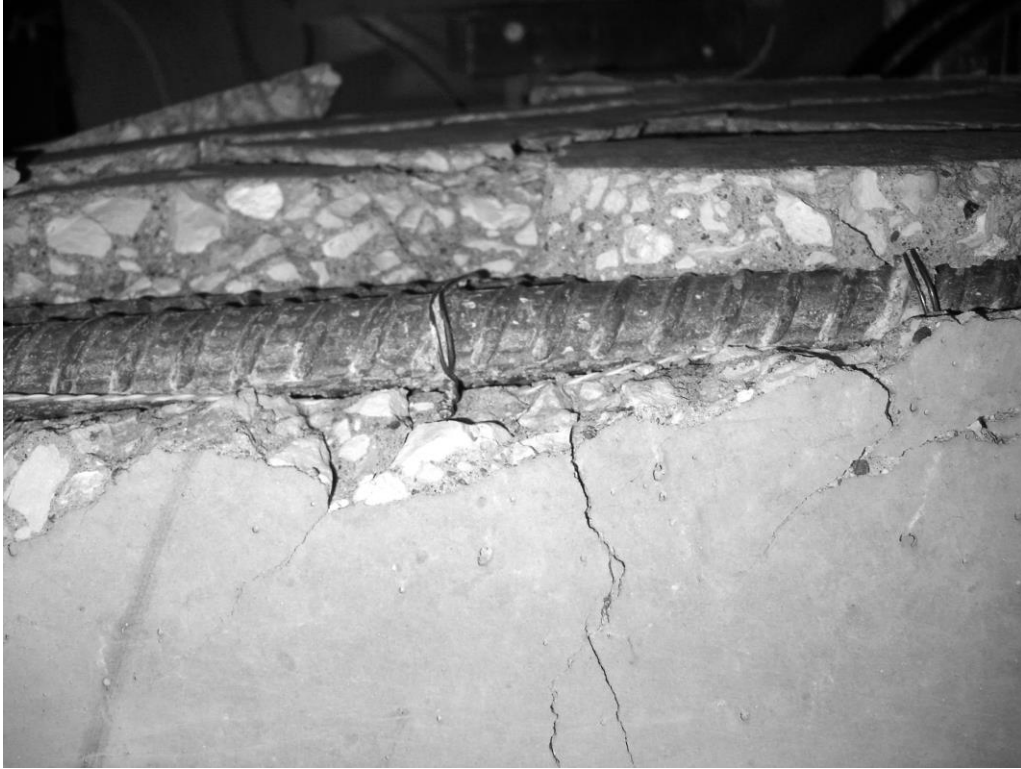


Figure 3.4 Crack pattern in constant moment region of series I

Beams with Steel Yielding Prior to Concrete Splitting - Series F-H with No.19 rebar and series L with No.25 rebar experienced limited steel yielding before the concrete cover split on the top and side faces of the beams. Like the previous series of specimens that failed in concrete splitting, flexural cracks were initiated in the splice region; both local concrete crushing at the rib-front area of black bars and strong adhesion between the enamel-coated rebar and concrete were observed. However, the beams with black steel reinforcement had fewer transverse flexural cracks in comparison with the previous series.

Overall, the beam specimens with coated rebar appeared to have a greater number of flexural cracks than those with black rebar. This observation indicated that the enamel-coated rebar can transfer stress more effectively due to a stronger steel-concrete bond. However, most flexural cracks of the two specimens with and without enamel coating occurred at similar locations of rebar termination.

3.3 Load-Deflection and Load-Strain Curves

To evaluate the effect of the enamel coating on the beam stiffness associated with the improved bond strength, the load-deflection and load-strain curves were compared in figures 3.5-3.10 for six pairs of representative beams. Overall, no significant difference in stiffness was observed before and after the ultimate load. This observation differed from the conclusion that enamel coating increased the pre-peak stiffness of pin-mortar specimens as a result of their improved bonding [13]. Adhesion between the enamel coating and cement was dominant in pin-mortar specimens, but relatively small in rebar-concrete specimens due to the significant bearing effect of bar deformation on concrete.

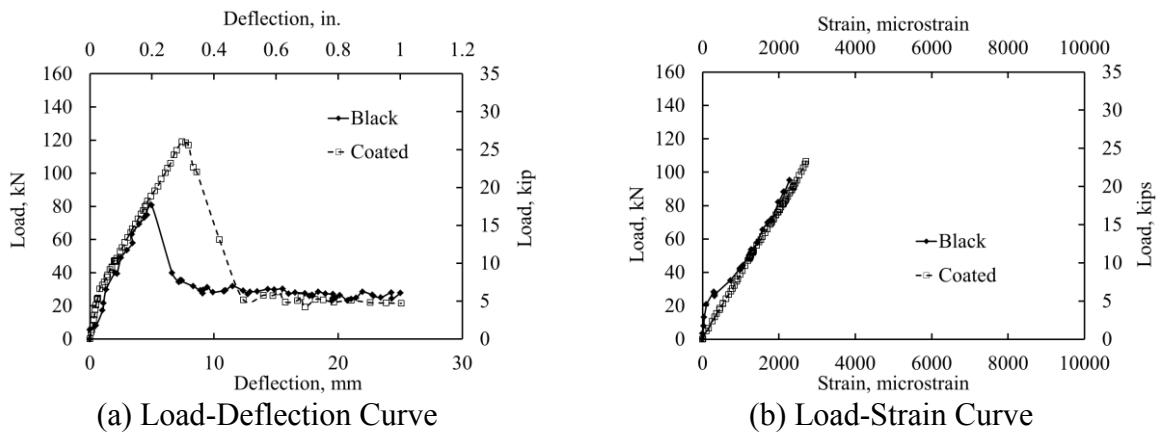
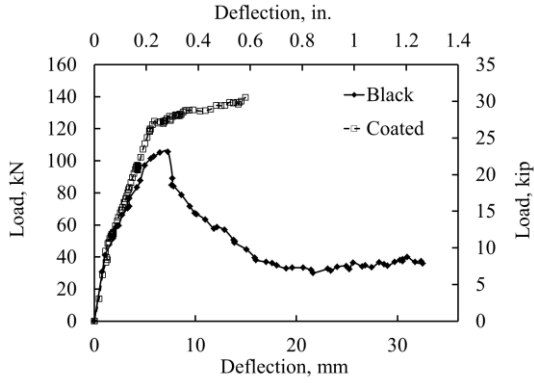
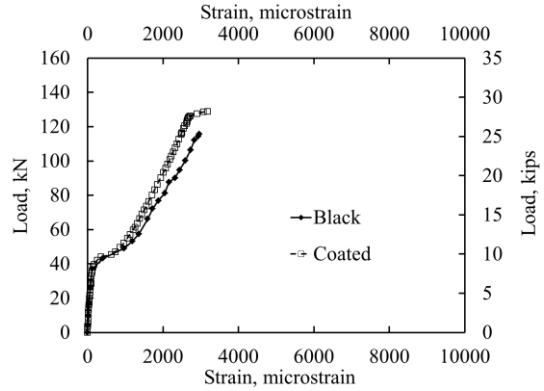


Figure 3.5 Load-deflection and load-strain curves for series C

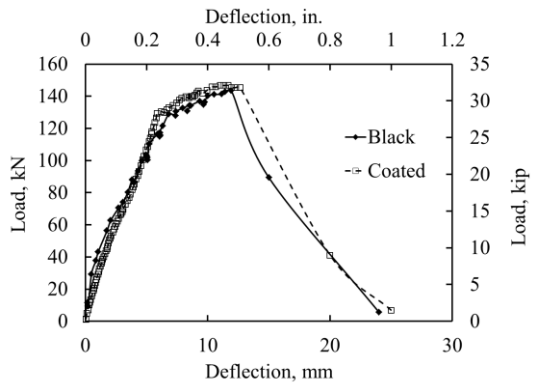


(a) Load-Deflection Curve

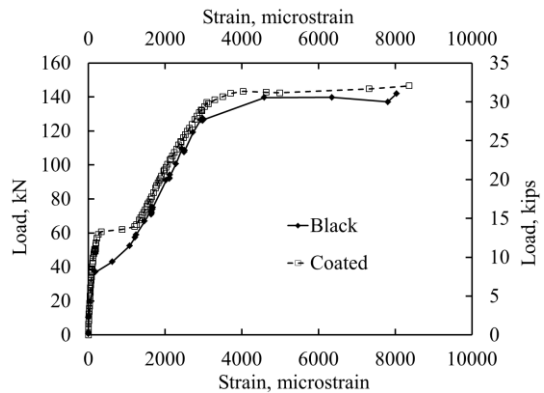


(b) Load-Strain Curve

Figure 3.6 Load-deflection and load-strain curves for series D

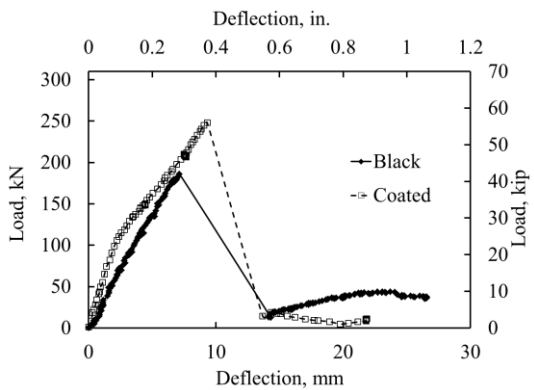


(a) Load-Deflection Curve

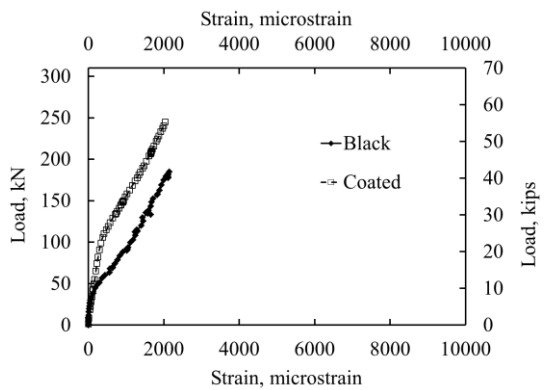


(b) Load-Strain Curve

Figure 3.7 Load-deflection and load-strain curves for series E

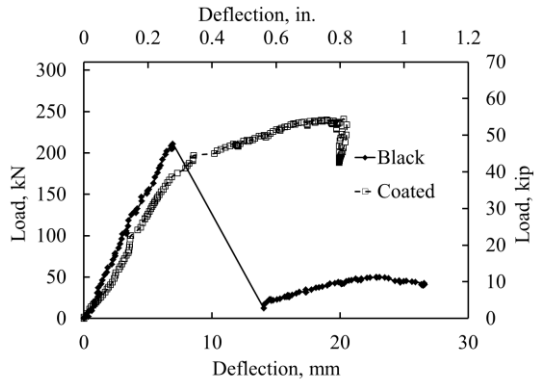


(a) Load-Deflection Curve

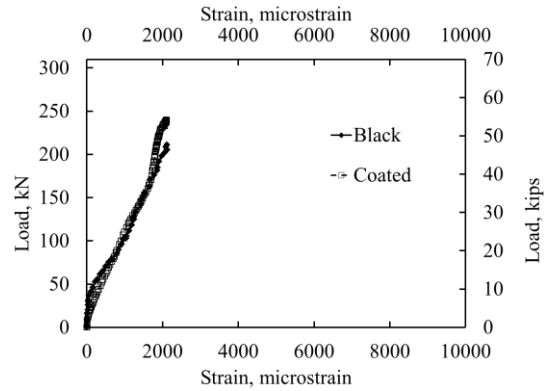


(b) Load-Strain Curve

Figure 3.8 Load-deflection and load-strain curves for series I

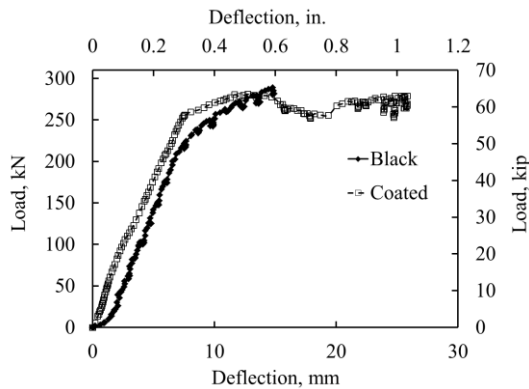


(a) Load-Deflection Curve

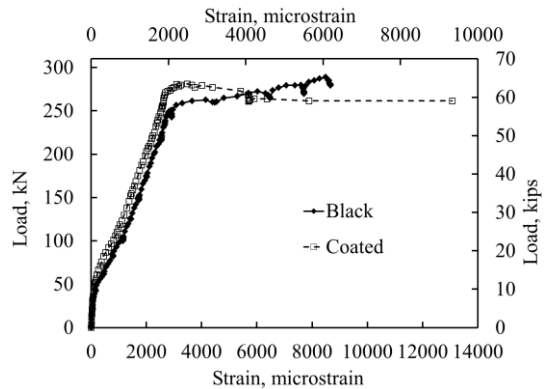


(b) Load-Strain Curve

Figure 3.9 Load-Deflection and Load-Strain Curves for Series K



(a) Load-Deflection Curve



(b) Load-Strain Curve

Figure 3.10 Load-Deflection and Load-Strain Curves for Series L

Beams with Concrete Splitting Failure – As shown in figures 3.5(a) and 3.8(a), as the beams were displaced gradually, the load increased linearly and rapidly at small displacement, continued to increase linearly at a reduced stiffness after concrete cracking, suddenly dropped at concrete splitting, and finally remained at a certain level mainly due to a friction effect. In comparison to the beams with black rebar, the beams with enamel-coated rebar endured larger deformation and a higher load due to the increased adhesion and friction of coated rebar in

concrete. As illustrated by the load-strain curves in figures 3.5(b) and 3.8 (b), no steel yielding was observed in the steel rebar.

Beams with Steel Yielding Prior to Concrete Splitting - With sufficient splice lengths, yield strength was eventually developed in the spliced bars, such as series F, G, H, and L. As represented by figure 3.10(a), a typical plateau was observed in the load-deflection curve. When the maximum load occurred after rebar yielding, the beams in each series had the same ultimate load resistance. The load-strain curves also confirmed the yielding of the steel rebar. In these cases, the maximum strain of the beams with enamel-coated rebar is significantly larger than that of black rebar, which indicates a more effective transfer of stress from the concrete to the coated steel rebar. For beams with slightly shorter splice lengths, as illustrated in figure 3.6(a) for series E, a limited degree of inelastic deformation was developed after initial yielding and the effect of the coating was insignificant.

Transition in Failure Modes - As the splice length increased, more stress was transferred from the concrete to the reinforcement. At the same splice length, the stress in the coated rebar was significantly higher than that of the black rebar. For example, figure 3.6(a) indicated that the maximum stress in the No.19 coated rebar spliced 406 mm in the confined beams was close to the yield strength, and the load-deflection curve showed the beginning of a yielding plateau. The load-strain curves in figure 3.6(b) confirmed the onset of initial yielding in the enamel-coated reinforcing rebar. However, the stress in the corresponding No.19 black rebar was significantly lower than the yield strength, and the load-deflection curve showed a sudden drop of load as concrete splitting occurred. Therefore, the enamel coating changed the structural behavior from a brittle concrete splitting failure to a nearly ductile steel yielding failure. A similar conclusion can

be drawn for the No.25 rebar spliced 1092 mm in the unconfined beams as illustrated in figure 3.9(a, b).

3.4 Bond Ratio

Splice Length Effect - The bond ratio for each series of two beams in pairs was calculated by dividing the ultimate bond strength of the enamel-coated rebar by that of the black rebar. As shown in figure 3.11, the calculated bond ratios were plotted as a function of splice length over rebar diameter ratio (l_d/d_b) for different confinement conditions. It can be clearly observed from figures 3.11 and table 2.1 that the bond ratios for all pairs of the beams tested in this experimental program are greater than or equal to 1.0. The bond ratio first increases at short splice lengths from 1.0 to a maximum value, such as 1.44, and then decreases to 1.0 when steel yielding occurs with long splice lengths. In theory, as the splice length approaches to zero, the bond strength is dominated by the strength of concrete between the two spliced rebar, becomes independent of coating conditions, and thus approaches 1.0. As indicated in figures 3.5, 3.6 and 3.8 for series C, D, and I beams, the maximum bond ratio corresponds to the maximum elastic stress that can be developed in the coated rebar, and lies in the range of 20 to 35 in splice length over rebar diameter ratio (l_d/d_b).

Confinement Effect – As shown in figure 3.11, beams with confined longitudinal rebar by transverse stirrups have lower bond ratios, indicating a relatively smaller coating effect of a confined splice joint. This is because confinement increases the bond strength of black rebar more rapidly than that of enamel-coated rebar. However, as the splice length continued to increase, the stress in the spliced rebar was close to the yield strength; the effect of confinement on bond ratio gradually diminished.

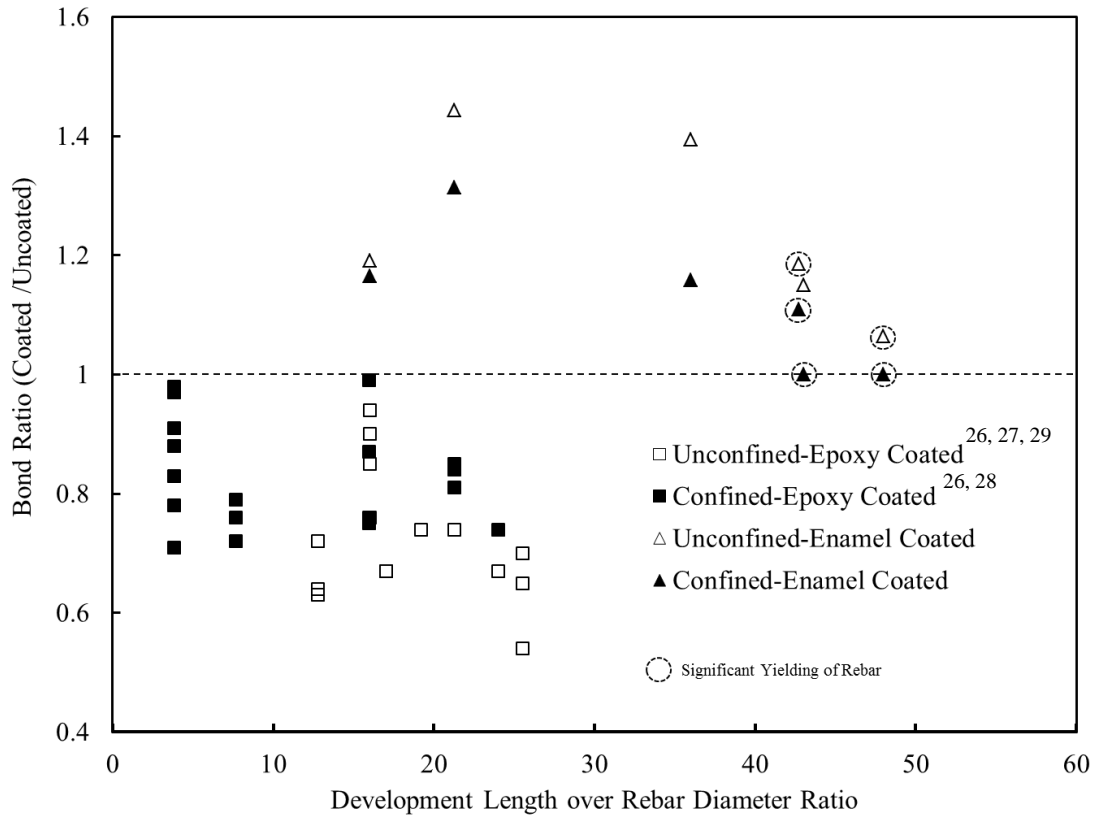


Figure 3.11 Bond ratio comparison between epoxy coated and enamel-coated rebar

Comparison with Epoxy Coated Rebar – Figure 3.11 also compares the bond ratios for enamel-coated rebar with those of epoxy-coated rebar that were collected from the literature [26-29]. While enamel coating increases the bond strength of steel rebar in concrete, the epoxy coating always reduces it. The bond ratio trend for epoxy-coated rebar with the splice length over rebar diameter ratio (l_d/d_b) appears a mirror image of that for enamel-coated rebar about a straight line of unit bond ratio at short splice lengths. With epoxy coating, the bond ratio of deformed rebar in concrete likely starts at 1.0 at short splice lengths, reaches a minimum value, and then goes back to 1.0 as the steel rebar begins yielding. Therefore, for practical designs, it is conservative to focus on the bond strength reduction of epoxy-coated rebar at $l_d/d_b = 20$ to 35 or

the bond strength increase of enamel-coated rebar at $l_d/d_b = 35$ to 43, towards initial yielding of steel rebar. As such, experimental studies on RC beams with long splice lengths are crucial.

3.5 Coating Factor for Enamel-Coated Rebar

To account for the coating effect, a coating factor was simply introduced into the existing relation between bond strength and development length in current design guidelines and codes (ACI 408R-03 [30] equation 4-11b, ACI 318-11 [8] equation 12-1, and AASHTO-11 [9] Article 5.11.2.1.1). These design equations were mainly based on elastic rebar data where short splice lengths were intentionally provided to achieve concrete splitting failures. Therefore, only the test results associated with the splitting failure in table 2.1 were used in this section. That is, the bond ratios for series A-D and I-K will be used in the following analysis, as presented in table 3.1.

It should be noted that Class B or C factors were not used in the calculation of bond strengths using either the AASHTO-11 or ACI 318-11 codes, as these factors are not for strength considerations, but reflect the brittle failure nature when all the splices are placed at the same location. The existing design equations from the aforementioned codes are applicable for epoxy-coated rebar after a coating factor of 1.2 or 1.5 has been introduced. For the enamel-coated rebar, the average bond ratio in table 3.1 is approximately 1.24, which corresponds to a coating factor of $1/1.24=0.81$. For design purposes, a conservative coating factor of 0.85 on the splice length is recommended, and its corresponding bond strength increased by an average factor of $1/0.85=1.176$ is much less than the value of 1.44 (Series C) achieved at near initial yielding of the rebar. The design bond strengths after using the design equation from each code multiplied by a factor of 1.176 are also listed in table 3.1. The means and standard deviations of the experimental to predicted ratios using various design specifications are presented in figure 3.12. It can be observed from figure 3.12 that the ACI 408R design equation with the proposed coating

factor gives the best prediction to the experimental data on both the average and standard deviation. Therefore, the development length for enamel-coated rebar splices can be obtained using the ACI 408R equation with a coating factor of 0.85.

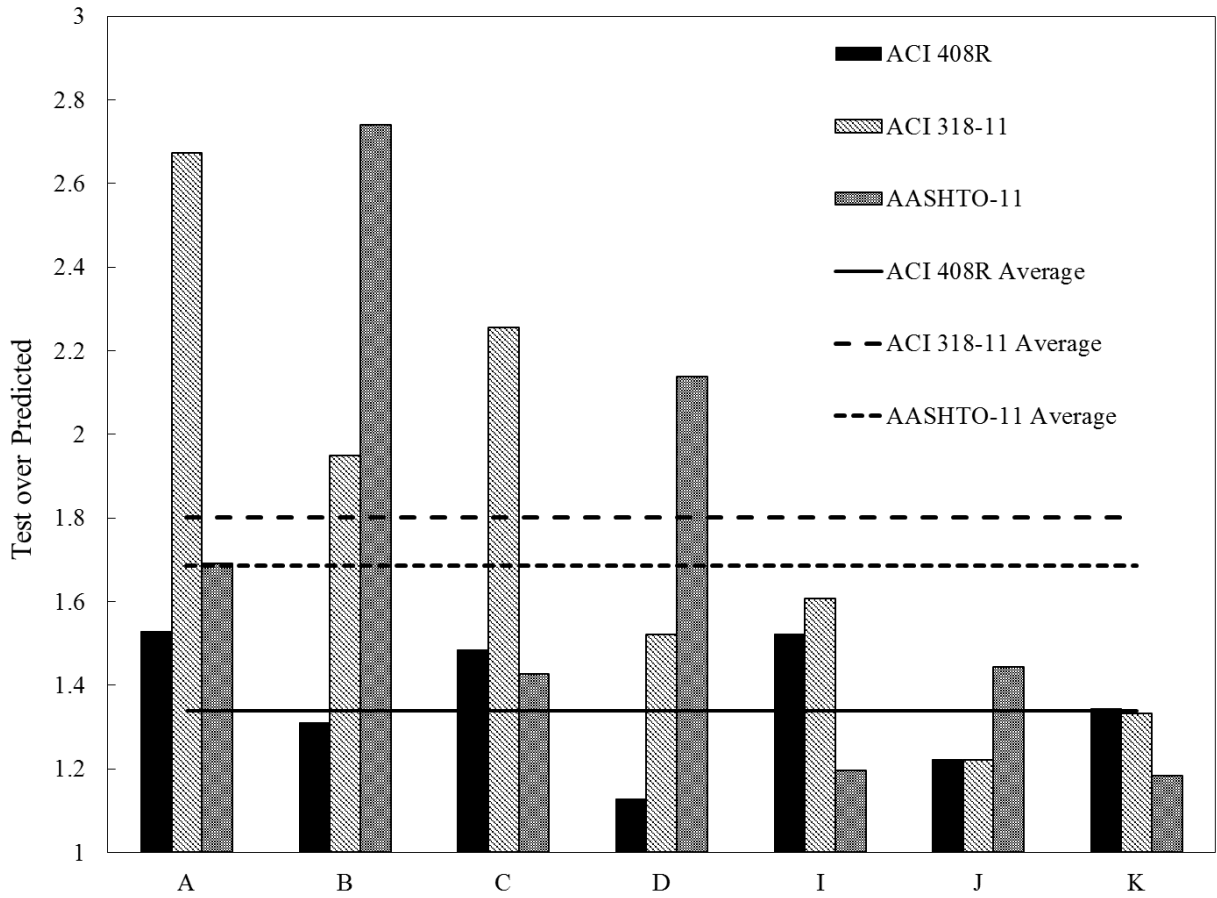


Figure 3.12 Ratio of test to predicted for series associated with splitting failure

Table 3.1 Bond Stress Prediction with Various Design Equations

Series	Notation	u_{avg} MPa	$u_{test,n}$ MPa	Bond Ratio	ACI 408R- 03 with 0.85 MPa	ACI 318-11 with 0.85 MPa	AASHTO-11 with 0.85 MPa	Test to Predicated ACI 408R-03	Test to Predicated ACI 318-11	Test to Predicated AASHTO-11
A	6C12N	5.33	5.49	1.16	3.59	2.05	3.24	1.528	2.674	1.691
B	6C12T	6.47	6.67	1.14	5.09	3.42	2.43	1.311	1.950	2.740
C	6C16N	4.49	4.63	1.44	3.12	2.05	3.24	1.484	2.255	1.426
D	6C16T	5.20	5.20	1.31	4.61	3.42	2.43	1.128	1.521	2.138
I	8C36N	3.33	3.43	1.35	2.26	2.14	2.87	1.522	1.607	1.195
J	8C36T	3.51	3.51	1.10	2.87	2.87	2.43	1.222	1.222	1.443
K	8C43N	2.77	2.85	1.15	2.12	2.14	2.41	1.344	1.333	1.184
Average Bond Ratio=1.24							Maximum:	1.528	2.674	2.740
Coating Factor=0.85							Minimum:	1.128	1.222	1.184
							Average:	1.339	1.801	1.686
							Standard Deviation:	0.159	0.481	0.528
							Coefficient of Variation:	0.119	0.267	0.313

Chapter 4 Conclusions

To evaluate the bond strength of vitreous enamel-coated rebar in normal strength concrete, 24 beam splice specimens were cast and tested. Based on the experimental results, the following conclusions can be drawn:

1. Enamel coating increases the bond strength of deformed rebar when spliced in normal strength concrete. As the splice length increases, the ratio of bond strength between coated rebar and black rebar first increases from 1.0 to a maximum value of 1.44 and then decreases to 1.0. The maximum bond strength ratio corresponds to a splice length over rebar diameter ratio of 20 to 35 when the maximum elastic stress is developed in enamel-coated rebar. The bond strength ratio approaches 1.0 both at zero splice length and at a very long splice length since the bond strengths in the two cases are governed by concrete splitting and steel yielding, respectively.

2. Confinement provided by transverse stirrups increases the bond strength of black rebar more rapidly than that of enamel-coated rebar. For enamel-coated rebar, an average of a 10% increase in bond strength was observed due to the confinement effect for a splice length over rebar diameter ratio of less than 20. For very long splice lengths, the stress in the spliced rebar (black or coated) is equal to the yield strength, and the confinement effect thus becomes negligible.

3. The increase in bond strength due to the coating is reflected mainly in the ultimate load of the structures or beams tested in this study; it has little or no influence on the pre- and post-peak stiffness of the beams. It is unlikely that the coating alters the distribution pattern of slip between the reinforcement and concrete.

4. The beams with coated steel rebar appear to have a greater number of smaller flexural cracks than those containing black rebar. This observation indicated that the enamel-coated rebar

more effectively transfers stress from the concrete to the rebar due to stronger steel-concrete bonding.

5. Enamel and epoxy coatings respectively increase and reduce the bond strength of deformed rebar in concrete. For practical designs, conservative coating factors should be developed in a splice length over rebar diameter ratio of greater than 35 for enamel-coated rebar and 20 to 35 for epoxy-coated rebar. It is critical to investigate the bond strength of enamel-coated rebar in concrete with long splice lengths, corresponding to initial yielding of steel rebar.

6. The ACI 408R design equation for splice length with a coating factor of 0.85 is recommended for design.

References

- [1]. Treece, R.A., and Jirsa J.O., “Bond Strength of Epoxy-Coated Reinforcing Bars,” PMFSEL Report No.87-1, Phil M. Ferguson Structural Engineering Laboratory, University of Texas at Austin, 85 pp., Jan. 1985.
- [2]. Johnston, D.W. and Zia, P., “Bond Characteristics of Epoxy Coated Reinforcing Bars,” Report No. FHWA-NC-82-002, Center for Transportation Engineering Studies, Civil Engineering Department, North Carolina State University, Raleigh, 163 pp., 1982.
- [3]. Choi, O.C., Hadje-Ghaffari, H., Darwin, D., and McCabe, S.L., “Bond of Epoxy-Coated Reinforcement to Concrete: Bar Parameters,” SL Report 90-1, University of Kansas Center for Research, Lawrence, 43 pp., Jan. 1990.
- [4]. Choi, O.C., Darwin, D., and McCabe, S.L., “Bond Strength of Epoxy-Coated Reinforcement to Concrete,” SM Report No.25, University of Kansas Center for Research, Lawrence, 217 pp., July, 1990.
- [5]. Choi, O.C., Hadje-Ghaffari, H., Darwin, D., and McCabe, S.L., “Bond of Epoxy-Coated Reinforcement: Bar Parameters,” ACI Materials Journal, V. 88, No.2, pp. 207-217, Mar.-Apr., 1990.
- [6]. Hadje-Ghaffari, H., Choi, O.C., Darwin, D., and McCabe, S.L., “Bond of Epoxy-Coated Reinforcement: Cover, Casting Position, Slump, and Consolidation,” ACI Structural Journal, V. 91 No.1, pp. 59-68, Jan-Feb., 1994.
- [7]. Idun, E.K. and Darwin, D., “Bond of Epoxy-coated Reinforcement: Coefficient of Friction and Rib Face Angle,” ACI Structural Journal, V.96, No.4, July-August 1999.
- [8]. ACI 318-11, Building Code Requirements for Structural Concrete, American Concrete Institute (ACI), Farmington Hills, MI, 2011.
- [9]. AASHTO-2011, LRFD Bridge Design Specifications, American Association of State Highways and Transportation Officials (AASHTO), Washington D.C., 2011.
- [10]. Tang, F.J., Chen, G.D., Brow, R.K., Volz, J.S., and Koenigstein, M.L., “Corrosion Resistance of Steel Rebar Coated with Three Types of Enamel,” Corrosion Science, Vol. 59, pp. 157-168, 2012.
- [11]. Day, D.C., Weiss, C.A., Malone, P.G., and Hackler, C.L., “Innovative Method of Bonding Portland Cement Concrete to Steel using a Porcelain Interface,” Proceedings of Materials Science and Technology (MS&T) Conference, Westerville, OH, The American Ceramic Society, 2006.

- [12]. Allison, P.G., Moser, R.D., Weiss Jr., C.A., Malone, P.G., and Morefield, S.W., "Nanomechanical and Chemical Characterization of the Interface between Concrete, Glass-ceramic Bonding Enamel and Reinforcing Steel," *Building and Construction Materials*, Vol. 37, pp.638-644, 2012.
- [13]. Yan, D.M., Reis, S., Tao, X., Chen, G.D., Brow, R.L., and Koenigstein, M.L., "Effect of Chemically Reactive Enamel Coating on Bonding Strength at Steel/Mortar Interface," *Construction and Building Materials*, Vol. 28, pp.512-518, Mar. 2012.
- [14]. Wu, C.L., Chen, G.D., Volz, J.S., Brow, R.K., and Koenigstein, M.L., "Local Bond Strength of Vitreous Enamel Coated Rebar to Concrete," *Construction and Building Materials*, V. 35, pp. 428-439, Oct. 2012.
- [15]. Tepfers, R., "A Theory of Bond Applied to Overlapped Tensile Reinforcement Splices for Deformed Bars," Publication No. 73:2, Division of Concrete Structures, Charlmers University of Technology, Goteborg, 328 pp.,1973.
- [16]. Orangun, C.O., Jirsa, J.O., and Breen, J.E., "A Reevaluation of Test Data on Development Length and Splices," *ACI Journal*, Vol.74, No.3, pp. 114-122., 1977.
- [17]. Canbay, E. and Frosch, R.J., "Bond Strength of Lap-Spliced Bars," *ACI Structural Journal*, V. 102, No. 4, pp. 605-614., July-August 2005.
- [18]. Darwin, D., McCabe, S.L., Idun, E.K., and Schoenekase, S.P., "Development Length Criteria: Bars not Confined by Transverse Reinforcement," *ACI Structural Journal*, V. 89, No. 6, pp. 709-720, Nov.-Dec., 1992.
- [19]. Zuo, J. and Darwin, D., "Splice Strength of Conventional and High Relative Rib Area Bars in Normal and High-Strength Concrete," *ACI Structural Journal*, V. 97, No. 4, pp. 630-641., July-August 2000.
- [20]. Esfahani, M.R., and Kianoush, M.R. "Development/Splice Length of Reinforcing Bars." *ACI Structural Journal*, Vol. 102, No. 1, Jan.-Feb. 2005.
- [21]. ASTM, Standard Specification for Deformed and Plain Carbon-Steel Bars for Concrete Reinforcement, American Society of Testing Methods (ASTM), A615/A615M, 2009.
- [22]. ASTM, Standard Test Methods and Definitions for Mechanical Testing of Steel Products, American Society of Testing Methods (ASTM), A370, 2010.
- [23]. Weiss, W.J., Guler, K., and Shah, S.P., "An Experimental Investigation to Determine the Influence of Size on the Flexural Behavior of High Strength Concrete Beams," *Proceedings of the Fifth International Symposium on the Utilization of High*

Strength/High Performance Concrete, Sandefjord, Norway, Vol. 1, pp. 709-718, 1999.

- [24]. Darwin, D., Tholen, M.L., Idun, E.K., Zuo, J., “Splice Strength of High Relative Rib Area Reinforcing Bars,” *ACI Structural Journal*, V. 93, No.3, pp. 95-107, 1996.
 - [25]. Cairns, J., and Abdullah, R.B., “Bond Strength of Black and Epoxy-Coated Reinforcement - a Theoretical Approach,” *ACI Materials Journal*, V.93, No.4, July-August, 1996.
 - [26]. Hamad B.S. and Jirsa J.O., “Strength of Epoxy-Coated Reinforcing Bar Splices Confined with Transverse Reinforcement”, *ACI Structural Journal*, V. 90, No.1, Jan.-Feb., pp. 77-88, 1993.
 - [27]. Treece, R. A., and Jirsa J.O., “Bond Strength of Epoxy-Coated Reinforcing Bars”, *ACI Materials Journal*, V. 86, No. 2, Mar.-Apr., 1989. pp. 167-174.
 - [28]. DeVries, R.A. and Moehle J.P., “Lap Splice Strength of Plain and Epoxy-Coated Reinforcement”, Department of Structure Engineering, Mechanics, and Materials, School and Civil Engineering, University of California at Berkeley, 1989, 117 pp.
 - [29]. Choi O.C., Hadje-Ghaffari H., Darwin D., and McCabe S. L., “Bond of Epoxy-Coated Reinforcement to Concrete: Bar Parameter,” University of Kansas Transportation Center, *Report No. 90-1*, Jan. 1990, 43pp.
 - [30]. ACI 408R-03., Bond and Development of Straight Reinforcing Bars in Tension, American Concrete Institute (ACI), Farmington Hills, MI, 2003.
-